



# Local features integration for content-based image retrieval based on color, texture, and shape

Mona Ghahremani<sup>1</sup> · Hamid Ghadiri<sup>2</sup> · Mohammad Hamghalam<sup>2</sup>

Received: 2 December 2019 / Revised: 14 February 2021 / Accepted: 1 April 2021 /  
Published online: 2 June 2021

© The Author(s), under exclusive licence to Springer Science+Business Media, LLC, part of Springer Nature 2021

## Abstract

Imaging techniques like computed tomography (CT) and ultrasound are employed to provide valuable information for physicians, including size, contour, and internal organs' anatomical information. Information retrieval systems can be used to deliver on-time information to the radiologists when some sections of scans are lost. In this study, a new content-based image retrieval (CBIR) model based on an effective combination of color, texture, and shape features is proposed to reconstruct these images' corrupted portions. For this purpose, image scans are normalized, and their noise is reduced by employing a median filter. Then, the color channel shift is modified utilizing the Simple Linear Iterative Clustering (SLIC) superpixel. Afterward, a Histogram of Oriented Gradients (HOG) descriptor is introduced to enhance image contrast and feature extraction. Finally, local thresholding based on Local Binary Patterns (LBP) is performed to separate the image details into three components to examine the light and edge intensity. The proposed method is experimented on several images by evaluating the texture, color, and shape morphology of the reconstructed images compared to the ground truth. The highest content retrieval rate of 90.54% on a liver CT scan image demonstrates the proposed method's efficiency compared with former state-of-the-art approaches.

**Keywords** Content-based image retrieval (CBIR) · Medical image processing · Morphology · LBP algorithm · HOG descriptor

---

✉ Hamid Ghadiri  
h.ghadiri@qiau.ac.ir

✉ Mohammad Hamghalam  
m.hamghalam@gmail.com

Mona Ghahremani  
monaghahremani1991@gmail.com

<sup>1</sup> Department of Control Electrical, Engineering, Darolfonoon University, Qazvin, Iran

<sup>2</sup> Faculty of Electrical, Biomedical and Mechatronics Engineering, Qazvin Branch, Islamic Azad University, Qazvin, Iran

## 1 Introduction

Although the content-based image retrieval has recently been a highly active research area, image complexity has led to many challenges. Many studies have been conducted to develop some algorithms for solving some issues, and they get the exact results when retrieving images and distinguishing between them. Image algorithms are employed by many of the proposed algorithms for extracting profiles and applying their properties to match similarities [38, 53].

Nevertheless, most algorithms use black and white images. Due to the need to retrieve the best images in large data, extensive research has been recently done on image retrieval. The first proposed ideas in the early 1970s were based on textual margins, regardless of their visual characteristics. Relevant images are available to users using their keywords. Accordingly, this is called text-based image retrieval [34]. The necessity of outsourcing such intensive image-characteristic detection tasks to cloud computing increasingly grows; however, when outsourcing it to a cloud platform, the concerns for the effective protection of private image and multimedia data is the major obstacle impeding the further implementation of cloud computing techniques over a lot of images and multimedia data [26]. A new scheme supporting Content-Based Image Retrieval (CBIR) is proposed over the encrypted images without revealing the sensitive information to the cloud server for addressing this challenge [32]. Several studies have focused on feature extraction for image retrieval. Various methods such as machine learning [25, 40], ontology-based methods [37, 38, 41], and wavelets [23, 24, 35, 39] are employed for this issue. The fundamental approach in CBIR is visual similarity. The similarity between feature vector values of different semantic categories reduces CBIR's performance since images are retrieved with no semantic relationship [50].

The systems mentioned above had some problems such as the margin squeeze that required a long time, high cost, and highly dependent on the designer's perception of the image. Furthermore, since the same image concepts are not the same from the various users' perspective, the boundaries attached to the images do not cover the whole issue; hence, the text-based queries are incomplete. CBIR is the required method in critical areas like medical science, industry, etc. Accordingly, image and video retrieval methods are discussed by Sundaram et al. ([51]), describing some methods as learned Lexicon-driven interactive video retrieval, a linear-algebraic technique with an application in semantic image retrieval, and logistic regression for image retrieval. Besides, Tyagi ([55]) introduced several strategies for bridging the semantic gap and reflecting recent CBIR advancements. LBP method, as an important one, is discussed in the study by Brahnam et al. [6], providing the latest literature reviews and some of the best LBP variants by researchers based on textual analysis research as well as research on LBP descriptors and variants. Moreover, the HOG method for image analysis is surveyed by Jahne [22] in some studies.

A new CBIR model based on an impressive integration of color, texture, and shape features is proposed in this paper to reconstruct the corrupted portions of these images. Image normalizing, denoising and color channel modifying by the SLIC superpixel method are the proposed algorithm's first steps. Afterward, the state-of-the-art techniques such as HOG, LBP, and HSV are applied to the dataset images. The combination of the texture, color, and shape morphology can improve the reconstructed images' retrieval performance compared to the ground truth. This work's main novelty is adopting well-known techniques to achieve high content retrieval rates for various applications such as clinical usages. The highest precision of 98.71% on a liver CT scan image exhibits the proposed method's efficiency.

The other innovations of this paper can be described as follows.

- The image will be normalized, and the noise reduction operation is conducted using the median filter
- The color channel is changed using the SLIC superpixel.
- Combinational usage of HOG and LBP algorithms for optimization

This paper uses image processing principles besides the median filter, HOG, SLIC superpixel, and LBP methods to determine the image pattern and its content-based image retrieval.

## 2 Literature review

In the early 1990s, with the size of the increased images in databases like the world wide web and to overcome the problems with text-based systems, the CBIR was proposed to automatically extract images and using visual concepts like color, texture, and shape of the images [8, 22, 30, 34, 51, 6, 55]. This era of digital technology has had a considerable share in medical sciences. The medical imaging modalities are rapidly growing in number due to the improvements in biomedical sensors and high-throughput image acquisition technologies [45].

Among the most used image retrieval systems, the Query By Image Content (QBIC) system developed by IBM, the Anaktisi [61], the image recovery system established by Columbia University called VisualSEEK, and the University of Amsterdam, called PicToSeek, may be referred to [57].

In medical applications, the fast growth of technology and the emergence of various imaging devices (MRI and X-ray and CT) have led to the introduction of CBMIR due to the growing production of medical images. Although content-based systems have been designed in many applications, only a small number of GoldMiner, IRMA, and ASSERT systems have been developed in the medical imagery area [17].

A bunch of CBMIR systems like high-resolution computed tomography (HRCT) lung images [12], mammography [27], chest CT [60], chest X-ray [44], spine X-ray [59], and dental X-ray [42] have considered the images of particular organs; these systems may not be applied to other medical devices. Due to the increased number of medical images, retrieving them in various applications like the effective detection of disease, research, education, and medical education will be very significant. As observed in Fig. 1, a content-based retrieval system forms the axis of the image.

### 2.1 Retrieval-based color features

Problems with effective search and navigation through the data can be solved by information retrieval. CBIR is a technique that helps search user-desired information from a huge set of image files and interpret user intentions for the desired information. The retrieval of information is based on image features like color, shape, texture, annotation, etc.

A color histogram is the most important color display used in image retrieval. Histogram sharing, comparisons, and coherent color histograms are known as the most important techniques used in this color display (to diminish the effects of noise). Moreover, other views are used for color features to retrieve images. For instance, colored moments and colored sets may be referred to [15, 18, 19].

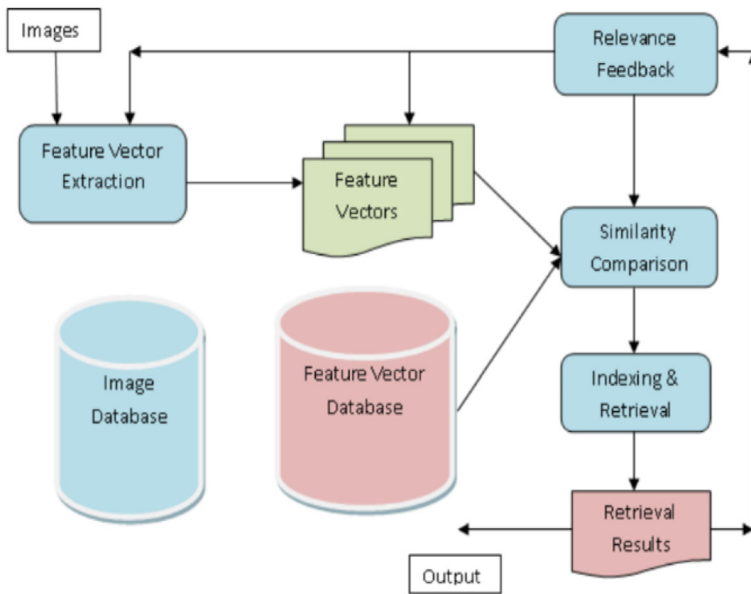


**Fig. 1** Content-based image retrieval system sample

The recovery-based color scheme feature refers to using color only on databases with high images that will significantly increase the number of incorrect returns and make this feature ineffective [47]. Thus, the color layout feature (the combination of color and spatial relationship of pixels) is proposed. This method's basic goal is to extract color specifications under some image areas, using color attributes in four-dimensional trees [16]. Image segmentation and using color property in each area may lead to very accurate results and increase the work's complexity.

The following are from other approaches addressed this issue: Using three first-color torques in some pixels in several predefined overlapping areas. This method works according to the distinction between pixels similar and non-similar to each area to the color of that area [4]. Whereas spacing layouts may be used with other features (like texture, etc.)

## 2.2 Retrieval-based texture features

The texture includes the visual patterns that cannot be displayed by color. There are different models for displaying and using textures. Recycling based on texture is not very effective. Nevertheless, it is better to use texture similarity between points of the same color (such as sky and sea, or leaves and grass). There is a variety of techniques for recognizing texture. A coincidence matrix is one of the first attempts in this field, with a background highly related to the issue of image retrieval [20]. Tamura method is one of the most important strategies in this area based on psychological studies and contextual texture features. The most critical techniques for texture retrieval operate according to quadratic value statistics comparisons between query items and database data. One can measure the image texture properties such as contrast, roughness, texture, or periodicity, and the patterns' randomness through these statistics [21]. Other approaches to the assessment of texture include wavelet transforms, Gabor filters, and fractals. There have been many papers presented on the efficiency of these methods in image processing applications.

## 2.3 Retrieval-based image form

The recovery-based form is the most intuitive retrieval form [36]. The most important feature making the form feature suitable for image processing applications is that a way may be resistant to transitions, rotations, and changes in its equivalence level. In these methods, some feature attributes of objects within images (independent of the direction and the map) are stored for each image and retrieved from them. Based on how they are extracted, form characteristics are divided into two categories of features based on edges and the regions [3]. The templates' elasticity, the finite element method, the comparison between the histogram of the image edges, and the skeletal representation of image objects compared with the graph matching conventions, the invariant functions, and wavelet descriptors are from the other consecutive methods proposed to accommodate forms. In this regard, an image content recovery method is presented using the HOG descriptor plus the superpixel SLIC along with the LBP (Ke [31]). It is noteworthy that a comparison with the other similar papers is conducted in terms of texture, color, and form.

## 3 Recent works

Several papers have been proposed in the area of content-based image retrieval. The measurement method is presented as a retrieval method for the image axis content in the study by (Mutasem K [1]) based on evolutionary algorithms. Two genetic algorithms are combined, and local searches are repeated as an image retrieval method. Also, in the study by [49], a quick content-based image retrieval method uses extensive data. The approach suggested by this study is to employ a hybrid algorithm called the Chain Clustering Binary Search Tree (CC-BST) that uses mapping reduction and Hadoop methods. In the research [56], the visual and pattern information of images is proposed using the kernel method to retrieve content-based image retrieval that represented recovery in large data based on linear mapping and encryption. In the study (Mutasem K [1]), the Memetic algorithm is applied for the content-based image retrieval of large data. This approach employed a genetic and large deluge algorithm representing the ability to restore images at the end of the work.

In the work of [13], a cellular neural network is utilized to repair the image. The use of this feed-forward network might restore a significant part of the damaged image. This kind of network may move from the cell to the cell in parallel (simultaneously with its neighbors and, the KNN method, or the nearest neighbors), leading to the rapid problem solving and learning rate. This project has been used for edge detection by averaging the cellular neural network. The network would learn how to specify the damaged edges. In the study by [58], a pre-trained deep neural network approach is employed along with an automatic noise reduction decoder to restore the image. This is a non-learning method, and the paper's approach is compared with the KSVD method. One of the basic weak points of this method is that the images with Gaussian noise could be better eliminated than other types like peppermint.

A model named Allen Kahn is applied in work by (Yibao [28]) to repair the images. This is a local method only applied to the domain and the two attributes. The first feature included the number of pixels in the repair domain collected by the curvature of the dissemination besides the use of image information outside the image restoration area, while the second one is the value of the outer pockets of the restoration like the damaged input area, which has not yet been processed on the same areas. The nonlinear equations

are used to solve this problem. That was why the program would function optimally. In [14], the self-organizing neural network or Kohonen mapping is employed for repairing the damaged digital images. In this study, this neural network's weak point is the need to set the algorithm parameter. A self-organized neural network is utilized to separate and repair the images as two separate networks. The MPEG-7, revealed by the Moving Picture Experts Group (MPEG), proposes a complete set of multimedia descriptors to create so-called descriptions that can be utilized by applications that allow quality access to content. MPEG-7 can support various applications and suggests reasonable storage, searching, and retrieval. In MPEG-7 based methods, Pattanaik et al. [46] proposed using a colour structure descriptor for the histogram of colour and edge. They combined these features to increase the performance of CBIR. However, their method was adapted and evaluated in computer vision applications. In this paper, we focus on CT scan images in medical applications. We adopt state-of-the-art algorithms in our clinical domains consist of ultrasound images and CT scans. Our contribution can be summarized as 1) We proposed a pipeline (shown in Fig. 2) based on HOG, LBP, and HSV to improve retrieval performance in CT-images 2) We evaluate the proposed model in our clinical applications (liver CT-scans).

## 4 The proposed method

Feature extraction methods may be used for characteristics like color, texture, and form. Image segmentation makes it possible to interact with the location parameter to extract the texture's color properties. i.e., in the case of segmentation, one may specify that the properties belonged to an area in the image correspond to and compared with the characteristics of the corresponding area of the alternative characteristics of images. In this structure, as described in the following, the segmentation method is employed to compare the areas beside the image's extraction of objects. The following sections will describe each of these methods.

### 4.1 SLIC super-pixel

Various segmentation methods have been used for investigating the semantic meanings of an image. The great performance and simple structure are the main reasons that cause the wide application of the SLIC method in image segmentation (Y. [33]). This algorithm is utilized for isolating a set of fractions, considering the intensity and spatial features. For filtering out the non-mass candidates, a selection rule is used [9].

That is to say; a simple method is used: Super-pixels, applying each image to about 25–200 regions. This method has many desirable features, as follows:

- 1) Reducing the images' complexity from thousands of pixels to just a few hundred pixels
- 2) Each superpixel is a perceptual constant, i.e., all pixels may be united in color and texture
- 3) Since pixels result from a general segmentation, most structures in the image are preserved.

Most algorithms used in computer models benefit from network pixels as a segmentation method. A simple duplicate clustering algorithm that conducts clustering in a five-dimensional space specified by the CIELAB color space's LAB values. SLIC is easy to use, and it can easily be employed practically; indeed, it is the only parameter determining the desired number of superpixels [9].

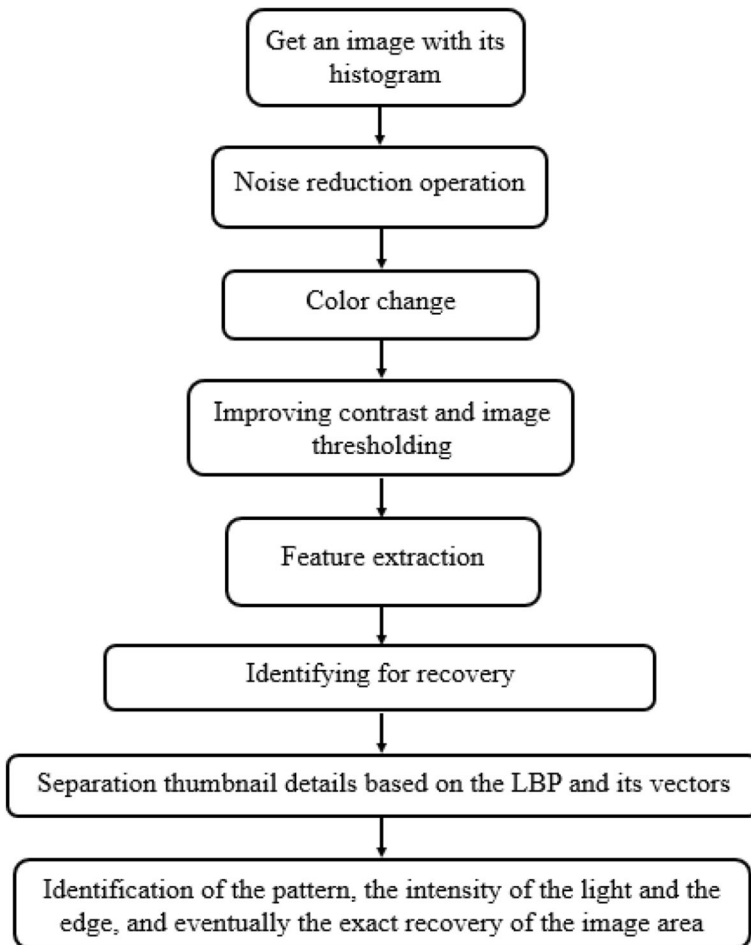


Fig. 2 The block diagram of the proposed method

## 4.2 HOG descriptor

Dalal and Triggs proposed a histogram of oriented gradients or HOG that is an interesting point of this descriptor to measure the distribution of gradient intensity or edge directions in the local region of an image [11]. The image is first transformed into fine-grained cells, and then a histogram collects steep directions or edge directions for pixels inside the cell for each region. A local character descriptor has resulted from the combination of these histograms. In this regard, the HOG descriptor is extracted from the full image before partitioning the image since the HOG attribute is extracted from the block, and transmitting the local information to the local description [54].

## 4.3 Color histogram

Over the past decade, color may be the most effective visual characteristic widely investigated in image retrieval research (Zhuohua [32]). A color histogram is proposed by Swain and

Ballard [52]. The distance between the two images is then measured by the histogram cross-section method as a straightforward method to take advantage of a decent function. However, its major drawback is that it is not strong enough for significant apparent variations, since it does not have any spatial information. That is the reason it has a local color descriptor [5]. There are multiple color spaces of RGB, HSV, YCrCb to interpret the color of an image. The color space used here is HSV, developed to provide an intuitive presentation of color to establish a simple way for humans to use colors skillfully. The HSV color model is more similar to the human perceptual understanding of colors since it decouples chromatic components from achromatic components, allowing humans to identify pure colors [48]. The color H shows the dominant component of the spectral color in its form in green, yellow, and red. Adding white color to pure color may lead to a color change; more color saturation will be obtained from less white. While the color’s brightness is shown by the amount (V), (S) indicates the saturation. Equation (1) represents the color histogram with HSV color mode.

$$\begin{aligned}
 V &= \max(R, G, B) \\
 S &= \begin{cases} \frac{V-\min(R, G, B)}{V} & \text{if } V \neq 0 \\ 0 & \text{Otherwise} \end{cases} \\
 H &= \begin{cases} \frac{60(G-B)}{V-\min(R, G, B)} & \text{if } V = R \\ 120 + \frac{60(B-R)}{V-\min(R, G, B)} & \text{if } V = G \\ 240 + \frac{60(R-G)}{V-\min(R, G, B)} & \text{if } V = B \end{cases} \tag{1}
 \end{aligned}$$

#### 4.4 Local binary patterns (LBP)

The Local Binary Patterns or LBP was introduced by [43] in the 1990s. The LBP feature extraction is efficient, and it can be obtained by multi-scale and non-invariant filters rather than scaling and rotation. Because of its invariance for lighting conditions and robustness for image noise, LBP has exhibited remarkable discriminative power in different domains. For instance, LBP has been employed in face recognition, multi-object tracking, as well as scene classification [10]. The idea behind this text manipulator is assigning a grayscale to each pixel code. The gray level ( $P_c$ ) corresponds to the coordinates ( $X_c, Y_c$ ) with adjacent portions ( $P_n$ ) employing the Eq. (2).

$$\begin{aligned}
 LBP(X_c, Y_c) &= \sum_{n=0}^P s(P_n - P_c) \\
 s(P_n - P_c) &= 1 \text{ if } P_n - P_c \geq 0 \\
 s(P_n - P_c) &= 0 \text{ if } P_n - P_c < 0
 \end{aligned} \tag{2}$$

where  $P$  stands for the number of adjoining pixels, generally, the neighborhood is considered  $3 \times 3$ , where  $P$  is equal to eight adjacent. Therefore, the LBP values varying between 0 and 255 for each pixel, as for an image for a grayscale. To form the LBP descriptor, a histogram based on these values is computed. A uniform LBP is used for this descriptor, extracting most of the basic structure of LBP. An LBP descriptor is considered the same if it has a maximum of 2 to 1 or 1 to 0 variations. For instance, both 00001000 (2 changes) and 1,000,000 (1 change) patterns are identical due to the maximum of two changes between 0 and 1 has occurred.



On the other hand, the pattern 01010010 is not the same; because it has six changes from 0 to 1 and 1 to 0. Therefore, the nine homogeneous patterns have a  $U$  value with a maximum value of 2 (0000000, 0000001, 0000011, 0000111, 0001111, 0011111, 0111111, and 1,111,111). These nine patterns correspond to 58 patterns out of 256 original rotated patterns, which may occur in  $3 \times 3$  regions. The remaining patterns accumulate in a single compartment, leading to a 59-chamber histogram. The use of only 58,256 of the template information may seem a waste of information; however, this approximation is supported by a significant observation. For instance, the nine chosen patterns appear to be the most convergent spatial patterns existing in algebraic microstructures.

### 4.5 Data extraction

This method has been proposed to use the powerful rating of descriptors mentioned above and overcome their limitations: HOG descriptor is first extracted from the entire image since it presents the shape’s local attribute. Subsequently, each image is divided into different sections. There are 16 sections for minimizing the density of information. Then, each section is rounded to extract and combine the HSV color and the LBP uniform histogram in a loop; however, the similarity between vectors is based on the calculation of Euclidean distance that is very optimal for comparing histograms and vectors.

### 4.6 Steps of proposed method

Extraction and combination of the local features through the proposed method in a single image

- Step 1: HOG descriptor is extracted from the entire image:  $V_{HOG}$
- Step 2: SLIC Superpixel is employed for the image to get 16 sections.
- Step 3: A round of each Superpixel creates a loop, and its edge is obtained.

- A) The rectangular ROI is calculated.
- B) To obtain local attributes, they are transmitted to descriptors.
- C) Conversion of the section to HSV space and obtaining the color histogram:  $V_{HSV_i}$
- D) Conversion of the section to gray and obtaining LBP feature:  $V_{LBP_i}$
- E) The two vectors are combined with Eq. (3)

$$\begin{aligned}
 V_{cmd1} &= V_{HSV1} + V_{LBP1} \\
 &\vdots \\
 &\vdots \\
 V_{Cmd16} &= V_{HSV16} + V_{LBP16}
 \end{aligned}
 \tag{3}$$

- Step 4: the color and texture descriptors are connected to obtain a local visual property by Eq. (4).

$$V_{CMD} = \{V_{CMD1}, V_{CMD2}, V_{CMD3}, \dots, V_{CMD16}\}
 \tag{4}$$

The vector is multiplied by the factor, and the characteristic of the form is added by Eq. (5).

$$V_{image} = V_{HOG} + W1 * V_{CMD} \quad (W1 = 0.3)
 \tag{5}$$

A visual investigation system created each dataset image's visual properties as a vector with numerical values stored in the data file to assess the described methods. According to the Euclidean distance, the query image property would be compared with the file's properties. Then, it would return images with a minimum distance of zero to monitor the query image. Precision and reminder parameters are commonly employed for calculating the quality of the imaging system in the image research system. The set of all relevant image results for each intended query is represented by  $A$ , and  $B_i$  stands for all the image results returned to the system. Accuracy may be defined as the percentage of the recovered images from the same section as the query image with Eq. (6).

$$P_i = \frac{A_i \cap B_i}{B_i} \quad (6)$$

This system has been designed to return 16 images after a query image; for each query, the address resolution protocol (ARP) is calculated by Eq. (7).

$$ARP = \frac{1}{N} \sum_{i=1}^N P_i \quad (7)$$

where  $N$  is the test portion in the dataset.

The Pseudo-code of the presented method is presented in Algorithm 1.

**Algorithm 1.** Pseudo-code of the presented method.

**INPUT:** *Images*

**OUTPUT:** *HistogramRetrivedImages*

$V_{HOG} = \text{extractHOGFeatures}(\text{image})$

$Slic_{sp} = \text{superpixels}(\text{image}, 16)$

**for**  $i=1:16$

$Mask(i) = \text{boundarymask}(Slic_{sp})$

$Roi(i) = \text{images.roi.Rectangle}(gca, 'Position', [ \dots, \dots, \dots, \dots ])$

$HSV(i) = \text{rgb2hsv}(Slic_{sp})$

$V_{HSV}(i) = \text{hist}(HSV(i))$

$RGB(i) = \text{rgb2gray}(Slic_{sp})$

$V_{LBP}(i) = \text{extractLBPFeatures}(RGB(i))$

$V_{cmd}(i) = V_{HSV}(i) + V_{LBP}(i)$

**end**

$V_{cmd} = \{V_{cmd}(1), V_{cmd}(2), \dots, V_{cmd}(16)\}$

$\text{HistogramRetrivedImages} = V_{HOG} + W_1 * V_{cmd}$

## 5 Experimental results

First, the dataset's input image needs to be inserted in the main dataset with multiple images in various areas, such as animal pictures, MRI images, CT scans, etc. The present approach is then tested on various data to assess its reliability in terms of the program's proposed method, model, structure, texture, color, and shape. The proposed CBIR model is implemented employing MATLAB R2018a (Mathworks Inc., Novi, MI, USA) on the platform Intel core i7-4720 @ 3.4GHz, 16G RAM, 64 bit.

For a better understanding of the proposed method, the block diagram is given below:

### 5.1 Datasets

Two datasets, including textual images, are employed in this study to evaluate the proposed method. The first dataset is IMAGENET1M, a dataset for large scale CBIR [7]. IMAGENET1M includes 2048-dimensional real-valued features gathered from a deep neural network model on a 10%-labeled ILSVRC-15 dataset. Base, query, training, and validation are four parts of this dataset in which both the 2048-dimensional features and the image list are provided. Li and Wang introduced the second dataset [29], composed of 10,000 test images. These images are stored in JPEG format with size  $384 \times 256$  or  $256 \times 384$ . Both of these datasets have several images in various fields.

### 5.2 Experiments

The initial input image is a CT scan that is an image of the liver with a distorted part of the liver's precise part.

**Step 1:** The input image is represented in Fig. 3, along with the image histogram.

**Step 2:** The image will be normalized in the following. At this stage, the noise reduction operation is conducted using the median filter, and the color channels change. Figure 4 is the result of the noise reduction operation using the median filter.

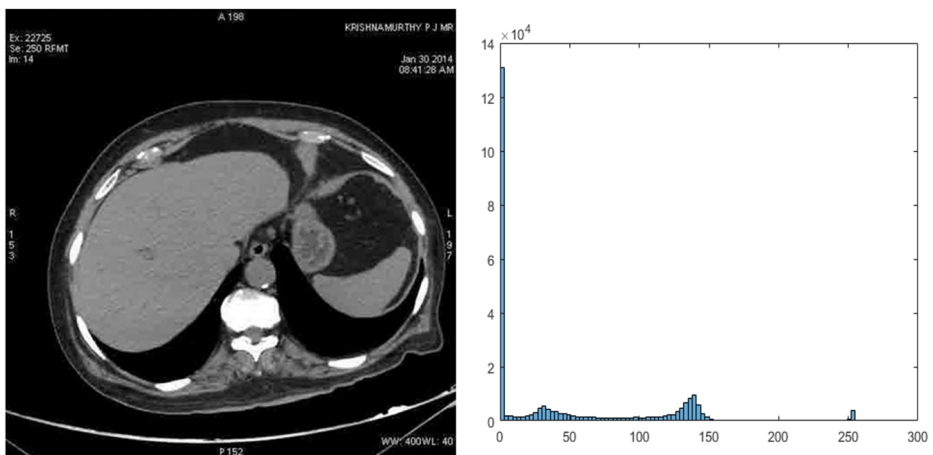


**Fig. 3** The input image and its histogram

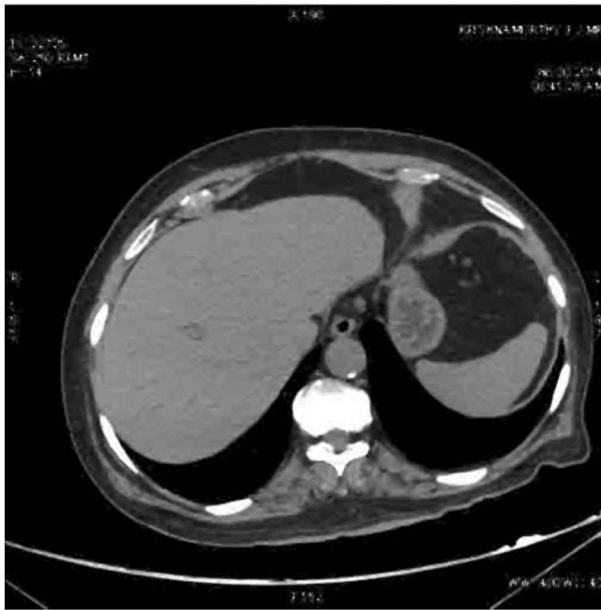


**Fig. 4** Noise reduction result by median filter

In fact, low pass filters have been applied to reduce noise in input images. The peak signal to noise ratio PSNR computed to determine the noise level after applying the median filter. Figure 4 illustrate the output image of the noise removal block.

**Step 3:** The color channel is changed using the SLIC superpixel. In this case, the red, blue, and green channels cover the image to see this section's output in Fig. 5.

**Step 4:** Contrast improvement and image thresholding are two necessary tasks to the distorted part that may be fully identified. In fact, the image is reconstructed, the row is

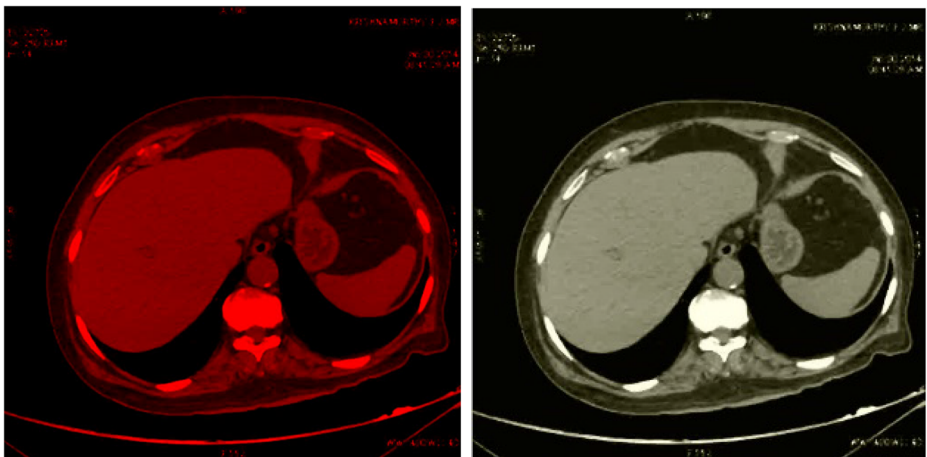


**Fig. 5** Changing color to red (left) and green channel (right)

selected, and the HOG descriptor is accomplished in the image. The output of this section is shown in Fig. 6.

**Step 5:** In the second phase, HOG should be conducted to extract feature, based on the two components of the light intensity and the edge of the image, to find the exact tampered segments. This is performed by the HOG descriptor, concurrently and repeatedly, until reaching the liver's object's exact edges. The output of this section is presented in Fig. 7.

For contrast, the edge information with the input image is combined to highlight the detected edge computed based on HOG. Specifically, strong points (corner) is selected to achieve high contrast images.

**Step 6:** Subsequently, the local threshold operations will be performed to identify the parts needed for recovery. Figure 8 presents its output.

**Step 7:** In this research, the thumbnail details separation in an image for retrieval is a significant point in content-based image retrieval systems according to LBP and its vectors. The main part in need of being retrieved should be identified as a template. This template is generally extracted based on the LBP and its vectors specified in the localization stage. Figure 9 presents the output of the detachable detail section in the image for image recovery.

**Step 8:** For retrieval with LBP and its vectors, the thumbnails in the image are separated into three phases, requiring identifying the pattern, the intensity of the light and the edge, and eventually, the exact recovery of the image area. The output of this content-based image retrieved section may be observed in Fig. 10.

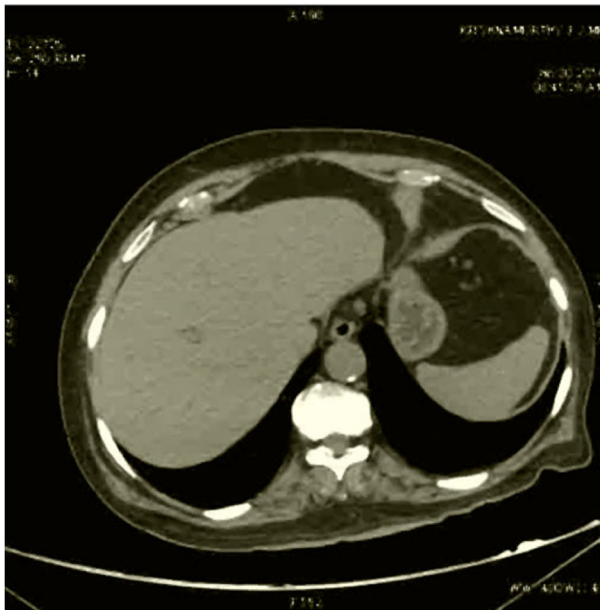


**Fig. 6** Image contrast enhancement and HoG thresholding in the initial extraction

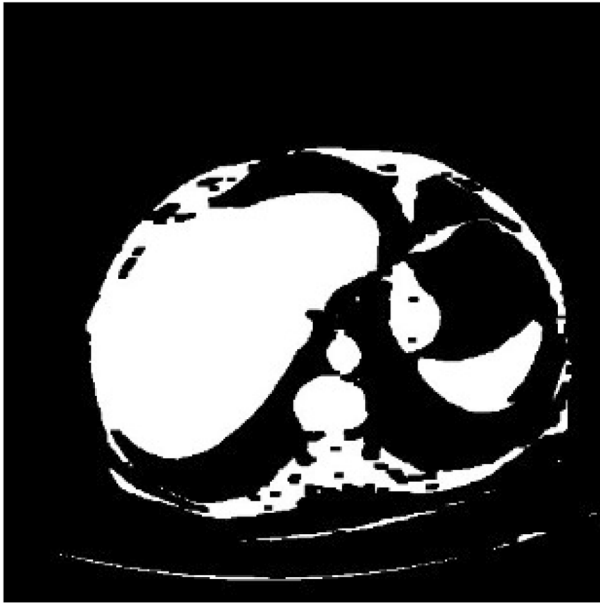


**Fig. 7** HOG feature extraction operation in second phased based on edge and light intensity

**Output:** Finally, the recovered image is in its original form, and its histogram is just like the original histogram, with the lowest variations, as in Fig. 11.



**Fig. 8** Local threshold operation

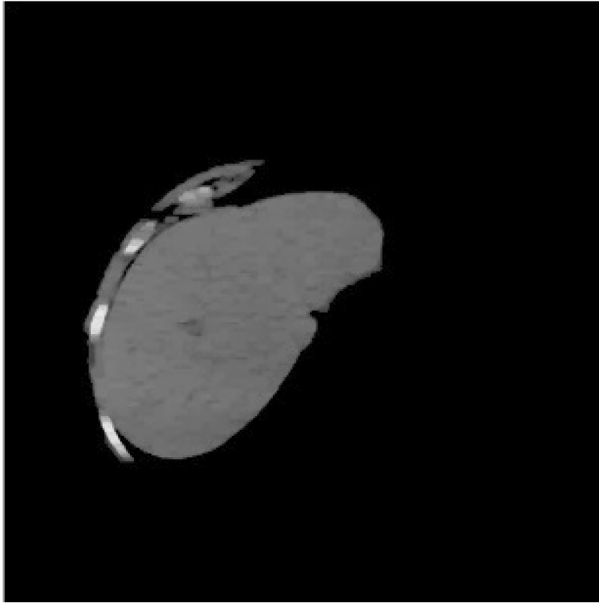


Fig. 9 Thumbnail detail separation for image retrieval based on LBP and its vectors

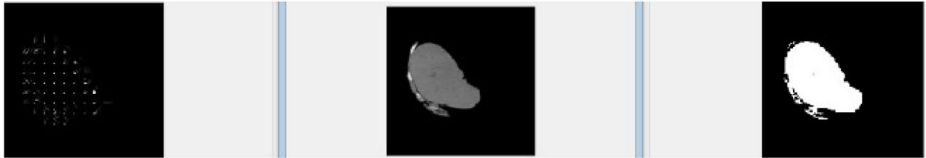


Fig. 10 From left to right: pattern recognition, light intensity, edge, and finally, precisely content-based image retrieval with LBP and its vectors

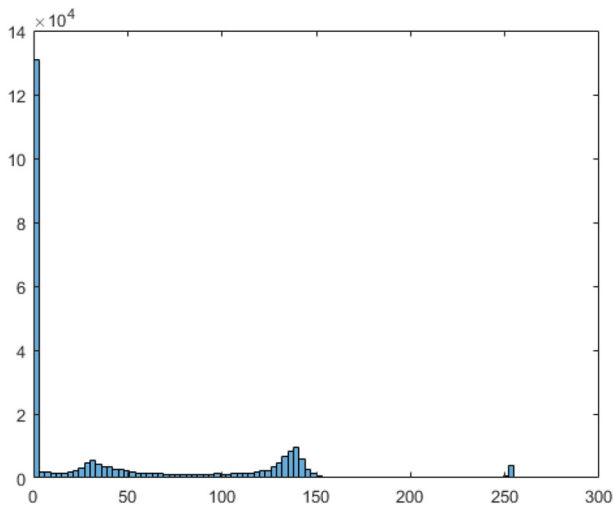


Fig. 11 Histogram of the retrieved image

**Table 1** The evaluation criteria result for a liver CT scan image

Recall (%)	Specificity (%)	Sensitivity (%)	Accuracy (%)	SNR (dB)	PSNR (dB)	MSE
90.54%	93.47%	95.20%	98.71%	32.14	45.54	0.1

**Table 2** Comparison of the proposed method with other approaches in terms of Accuracy and Recall

References	Recall (%)	Accuracy (%)
(Mutasem K. [2])	88%	88%
[49]	69.2%	83.5%
[56]	89%	97%
(Mutasem K. [1])	70%	88%
Proposed Method	90.54%	98.71%

The image's output by applying the liver image from the CT scan data collection and the animal image has good results. According to Section 4.5, the HOG descriptor is first extracted from the entire image. There are 16 sections for minimizing the density of information.

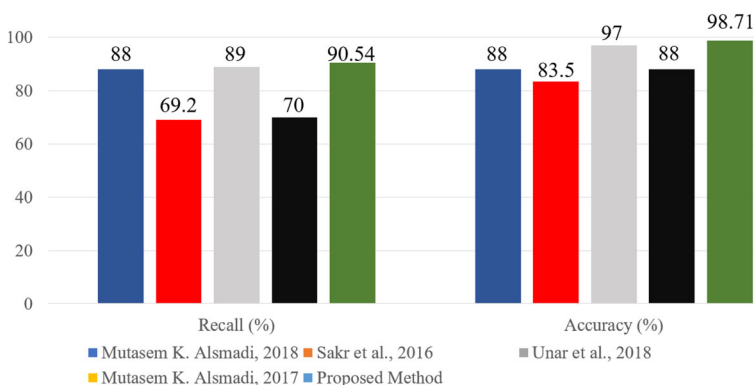
In the following, the evaluation criteria for the assessment of the proposed approach are to be determined, generally including evaluation results, as observed in Table 1.

As shown in Table 2, the criteria' comparison results are based on reference papers with different criteria measured in the same conditions.

Table 2 shows the accuracy and recall indices of the proposed approach compared to similar studies in the same conditions. Besides, the comparison between the evaluation terms of these papers and the proposed approach is demonstrated in Fig. 12.

## 6 Conclusion

CBIR is a technique for finding the images from large data that attracted much attention in the last decade. Extracting features may be associated with various image capabilities like color structure, image texture, etc. Nevertheless, the fundamental problem here is that the simple

**Fig. 12** Comparison of the proposed method with other approaches in evaluation terms



information checked by a computer has a lot to do with the deep understanding picked up by a person. In the present study, a new CBIR approach is suggested to reconstruct and improve the quality of the distorted images. A combination of color, texture, and shape features based on modifying the color channel using SLIC, enhancing the image contrast via HOG, and separating the image details applying LBP is proposed in this study. Experimental outcomes indicated that the proposed approach yielded higher retrieval accuracy than the other similar works. Obtained content retrieval rate of 90.54% and accuracy of about 98.71% on a liver CT scan image, illustrate the efficiency of the proposed approach.

## References

1. Alsmadi MK (2017) An efficient similarity measure for content based image retrieval using memetic algorithm. *Egypt J Basic Appl Sci* 4(2):112–122. <https://doi.org/10.1016/j.ejbas.2017.02.004>
2. Alsmadi MK (2018) Query-sensitive similarity measure for content-based image retrieval using meta-heuristic algorithm. *J King Saud Univ Comput Inf Sci* 30(3):373–381. <https://doi.org/10.1016/j.jksuci.2017.05.002>
3. Bazzani L, Cristani M, Murino VJCV (2013) Symmetry-driven accumulation of local features for human characterization and re-identification. *Comput Vis Image Underst* 117(2):130–144
4. Berens J, Finlayson GD, Qiu G (2000) Image indexing using compressed colour histograms. *IEE Proc Vis Image Sig Process* 147(4):349–355
5. Bianconi F, Bello-Cerezo R, Napoletano PJOEI (2017) Improved opponent color local binary patterns: an effective local image descriptor for color texture classification. *J Electron Imaging* 27(1):011002
6. Brahmam S, Jain LC, Nanni L, Lumini A (2014) *Local binary patterns: new variants and applications*. Springer
7. Cai D, Gu X, Wang C (2017) A revisit on deep hashings for large-scale content based image retrieval. *arXiv preprint arXiv:1711.06016*
8. Chang S-K, Hsu A (1992) Image information systems: where do we go from here?. *IEEE Trans Knowl Data Eng* 4:431–442
9. Chu J, Min H, Liu L, Lu W (2015) A novel computer aided breast mass detection scheme based on morphological enhancement and SLIC superpixel segmentation. *Med Phys* 42(7):3859–3869. <https://doi.org/10.1118/1.4921612>
10. Ciocca G, Cusano C, Schettini RJMT (2015) Image orientation detection using LBP-based features and logistic regression. *Multimed Tools Appl* 74(9):3013–3034
11. Dalal N, Triggs B (2005) Histograms of oriented gradients for human detection 2005 IEEE computer society conference on computer vision and pattern recognition (CVPR'05). IEEE, pp. 886–893
12. Dy JG, Brodley CE, Kak A, Broderick LS, Aisen AM (2003) Unsupervised feature selection applied to content-based retrieval of lung images. *IEEE Trans Pattern Anal Mach Intell* 25:373–8
13. Elango P, Murugesan K (2009) Digital image inpainting using cellular neural network. *Int J Open Probl Compt Math* 2(3):439–450
14. Favorskaya M, Jain LC, Bolgov A (2014) Image inpainting based on self-organizing maps by using multi-agent implementation. *Procedia Comput Sci* 35:861–870
15. Feng L, Li H, Gao Y, Zhang Y (2020) A color image segmentation method based on region salient color and fuzzy c-means algorithm. *Circ Syst Sig Process* 39(2):586–610
16. Gevers T, Smeulders AW (2000) Pictoseek: combining color and shape invariant features for image retrieval. *IEEE Trans Image Process* 9(1):102–119
17. Ghosh P, Antani S, Long LR, Thoma GR (2011) Review of medical image retrieval systems and future directions. 2011 24th International Symposium on Computer-Based Medical Systems (CBMS), pp 1–6
18. Hafner J, Sawhney HS, Equitz W, Flickner M, Niblack W (1995) Efficient color histogram indexing for quadratic form distance functions. *IEEE Trans Pattern Anal Mach Intell* 17(7):729–736
19. Han J, Ma K-K (2002) Fuzzy color histogram and its use in color image retrieval. *IEEE Trans Image Process* 11(8):944–952
20. Hiremath P, Pujari J (2007) Content based image retrieval based on color, texture and shape features using image and its complement. *Int J Comput Sci Secur* 1(4):25–35
21. Humeau-Heurtier A (2019) Texture feature extraction methods: A survey. *IEEE Access* 7:8975–9000
22. Jahne B (2004) *Practical handbook on image processing for scientific and technical applications*. CRC press

23. Jindal H, Kasana SS, Saxena S (2016) A novel image zooming technique using wavelet Coefficients Proceedings of the International Conference on Recent Cognizance in Wireless Communication & Image Processing. Springer, pp. 1-7
24. Kaur S, Jindal H (2017) Enhanced image watermarking technique using wavelets and interpolation. *Int J Image Graph Sig Process* 11(7):23
25. Kavitha S, Thyagarajan K (2015) Analysis of multimodality brain images using machine learning techniques 2015 Int Conf Commun Sig Process (ICCCSP). IEEE, pp. 1482-1486
26. Kavitha S, Thyagarajan K (2017) Efficient DWT-based fusion techniques using genetic algorithm for optimal parameter estimation. *Soft Comput* 21(12):3307–3316
27. Korn P, Sidiropoulos N, Faloutsos C, Siegel E, Protopapas Z (1998) Fast and effective retrieval of medical tumor shapes. *IEEE Trans Knowl Data Eng* 10:889–904
28. Li Y, Jeong D, Choi J-I, Lee S, Kim J (2015) Fast local image inpainting based on the Allen–Cahn model. *Dig Sig Process* 37:65–74
29. Li J, Wang JZ (2003) Automatic linguistic indexing of pictures by a statistical modeling approach. *IEEE Trans Pattern Anal Mach Intell* 25(9):1075–1088
30. Li X, Chen S-C, Shyu M-L (2002) Furht B. Image retrieval by color, texture, and spatial information. Proceedings of the 8th international conference on distributed multimedia systems, pp 152–9
31. Li K, Zou C, Bu S, Liang Y, Zhang J, Gong MJPR (2018) Multi-modal feature fusion for geographic image annotation 7:1–14
32. Liu Z, Huang C, Suo H, Yang B (2019) A novel content based image retrieval scheme in cloud Computing International Conference on Artificial Intelligence and Security. Springer, pp. 606-616
33. Liu Y, Yu M, Li B, He Y (2018) Intrinsic manifold SLIC: A simple and efficient method for computing content-sensitive Superpixels. *IEEE Trans Pattern Anal Mach Intell* 40(3):653–666. <https://doi.org/10.1109/TPAMI.2017.2686857>
34. Long F, Zhang H, Feng DD (2003) Fundamentals of content-based image retrieval. Multimedia information retrieval and management. Springer, pp 1-26
35. Mander K, Jindal H (2017) An improved image compression-decompression technique using block truncation and wavelets. *Int J Image Graph Sig Process* 9(8):17
36. Mehmood Z, Abbas F, Mahmood T, Javid MA, Rehman A, Nawaz TJAJFS (2018) Content-based image retrieval based on visual words fusion versus features fusion of local and global features. *Arab J Sci Eng* 43(12):7265–7284
37. Minu RI, Thyagarajan KK (2013) A novel approach to build image ontology using texton. *Intelligent Informatics*, Springer, 333–339
38. Minu R, Thyagarajan K (2014) Semantic rule based image visual feature ontology creation. *Int J Autom Comput* 11(5):489–499
39. Mittal A, Jindal H (2017) Novelty in image reconstruction using DWT and CLAHE. *Int J Image Graph Sign Process* 9(5):28
40. Nagarajan G, Thyagarajan K (2012) A machine learning technique for semantic search engine. *Procedia Eng* 38:2164–2171
41. Nagarajan G, Thyagarajan KK (2014) Rule-based semantic content extraction in image using fuzzy ontology. *Int Rev Comput Softw* 9(2):266–277
42. Nomir O, Abdel-Mottaleb M (2008) Hierarchical contour matching for dental X-ray radiographs. *Pattern Recog* 41:130–138
43. Ojala T, Pietikäinen M, Harwood D (1996) A comparative study of texture measures with classification based on featured distributions. *Pattern Recog* 29(1):51–59
44. Oliveira LLG, e Silva SA, Ribeiro LHV, de Oliveira RM, Coelho CJ, Andrade ALS (2008) Computeraided diagnosis in chest radiography for detection of childhood pneumonia. *Int J Med Inform* 77:555–564
45. Owais M, Arsalan M, Choi J, Park KR (2019) Effective diagnosis and treatment through content-based medical image retrieval (CBMIR) by using artificial intelligence. *J Clin Med* 8(4):462
46. Pattanaik S, Bhalke D (2012) Efficient content based image retrieval system using Mpeg-7 features. *Int J Comput Appl* 53:19–24
47. Qin C, Sun M, Chang C-C (2018) Perceptual hashing for color images based on hybrid extraction of structural features. *Signal Process* 142:194–205
48. Sajjad M, Ullah A, Ahmad J, Abbas N, Rho S, Baik SW (2018) Integrating salient colors with rotational invariant texture features for image representation in retrieval systems. *Multimed Tools Appl* 77(4):4769–4789
49. Sakr NA, ELdesouky AI, Arafat HJC (2016) An efficient fast-response content-based image retrieval framework for big data. *Comput Electr Eng* 54:522–538
50. Sharif U, Mehmood Z, Mahmood T, Javid MA, Rehman A, Saba T (2019) Scene analysis and search using local features and support vector machine for effective content-based image retrieval. *Artif Intell Rev* 52: 901–25

51. Sundaram H, Naphade M, Smith J, Rui Y (2006) Image and Video Retrieval. 5th Internatinoal Conference, CIVR 2006, Tempe, AZ, USA, July 13-15, 2006, Proceedings. Springer
52. Swain MJ, Ballard DH (1992) Indexing via Color Histograms. In: Sood AK, Wechsler H (eds) *Active Perception and Robot Vision*. 1992//. Springer Berlin Heidelberg, Berlin, Heidelberg, pp 261–273
53. Thyagarajan KK, Raji IK (2019) A review of visual descriptors and classification techniques used in leaf species identification. *Arch Comput Methods Eng* 26(4):933–960
54. Torrione PA, Morton KD, Sakaguchi R, Collins LMJITOG, Sensing R (2013) Histograms of oriented gradients for landmine detection in ground-penetrating radar data. *IEEE Trans Geosci Remote Sens* 52(3): 1539–1550
55. Tyagi V (2017) *Content-Based Image Retrieval*. Springer Nature
56. Unar S, Wang X, Zhang C (2018) Visual and textual information fusion using kernel method for content based image retrieval. *Inf Fusion* 44:176–187
57. Veltkamp RC, Tanase M (2000) Content-based image retrieval systems: A survey
58. Xie J, Xu L, Chen E (2012) Image denoising and inpainting with deep neural networks *Adv Neural Inf Process Syst*, pp 341–349
59. Xu X, Lee D-J, Antani S, Long LR (2008) A spine X-ray image retrieval system using partial shape matching. *IEEE Trans Inf Technol Biomed* 12:100–108
60. Yu S-N, Chiang C-T, Hsieh C-C (2005) A three-object model for the similarity searches of chest CT images. *Comput Med Imaging Graph* 29:617–30
61. Zagoris K, Chatzichristofis SA, Papamarkos N, Boutalis YS (2009) *img (Anaktisi): A web content based image retrieval system*. Proceedings of the 2009 Second International Workshop on Similarity Search and Applications: IEEE Computer Society, pp 154–5

**Publisher's note** Springer Nature remains neutral with regard to jurisdictional claims in published maps and institutional affiliations.